# Supplementary Information

# Fabrication of a Hybrid Cellularized Cardiac Patch via 3D Bioprinting of Alginate-Gelatin-PEOz Patterns on Electrospun PLCL-PEOz Nanofibers

**Muthu Parkkavi Sekar[1], David Raj Chellappan[2], Dhakshinamoorthy Sundaramurthi[1], Swaminathan Sethuraman[1]***

[1]Tissue Engineering & Additive Manufacturing (TEAM) Lab
Centre for Nanotechnology & Advanced Biomaterials
ABCDE Innovation Centre
School of Chemical & Biotechnology
SASTRA Deemed University, India

[2] Central Animal Facility (CAF)
School of Chemical and Biotechnology
SASTRA Deemed University, Thanjavur, India

---

***Corresponding Author**

**S. Swaminathan, Ph. D.**
Professor, Tissue Engineering & Additive Manufacturing (TEAM) Lab
Director, Centre for Nanotechnology & Advanced Biomaterials (CeNTAB)
ABCDE Innovation Centre
School of Chemical & Biotechnology (SCBT)
SASTRA Deemed University
Tirumalaisamudram, Thanjavur– 613 401
Tamil Nadu, India

Email: swami@sastra.edu

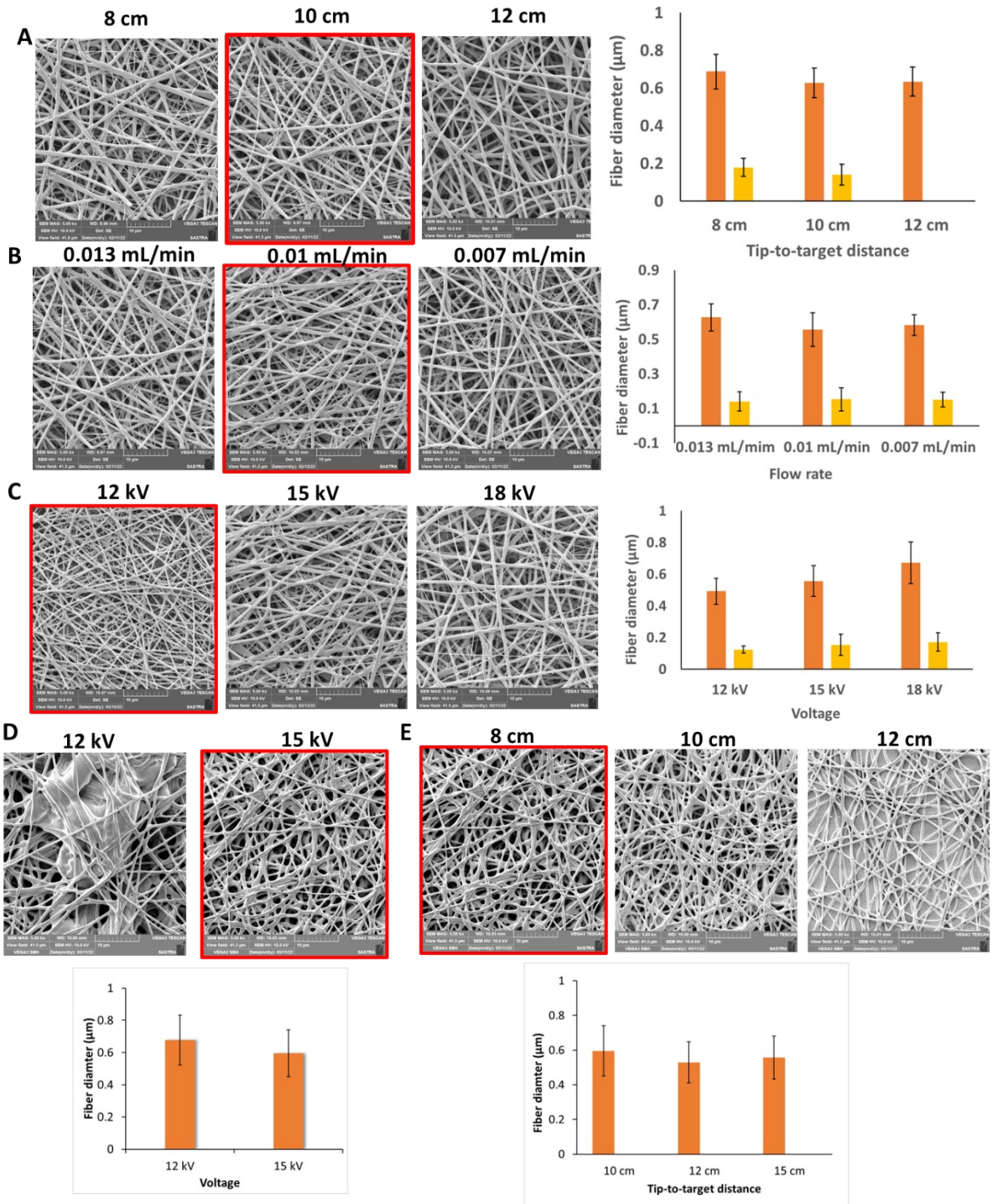


Figure 1 SEM images and fiber diameter distributions of electrospun B73 and PLCL random nanofibers. (A) B73 random fibers fabricated at varied tip-to-collector distances ( 8, 10 and 12 cm) with a constant flow rate of 0.013 mL/min and applied voltage of 12 kV. (B) B73 random fibers obtained by varying the flow rate from 0.013 to 0.007 mL/min, while maintaining a constant voltage of 12 kV and tip-to-collector distance of 10 cm. (C) B73 random fibers produced at different applied voltages (12, 15 and 18 kV) with a constant flow rate of 0.01 mL/min and a tip-to-collector distance of 10 cm. (D–E) SEM images and fiber diameter distributions of electrospun PLCL random nanofibers, fabricated at varied voltages (12 and 15 kV) and tip-to-collector distances (8, 10, and 12 cm) (scale bar: 10 µm).

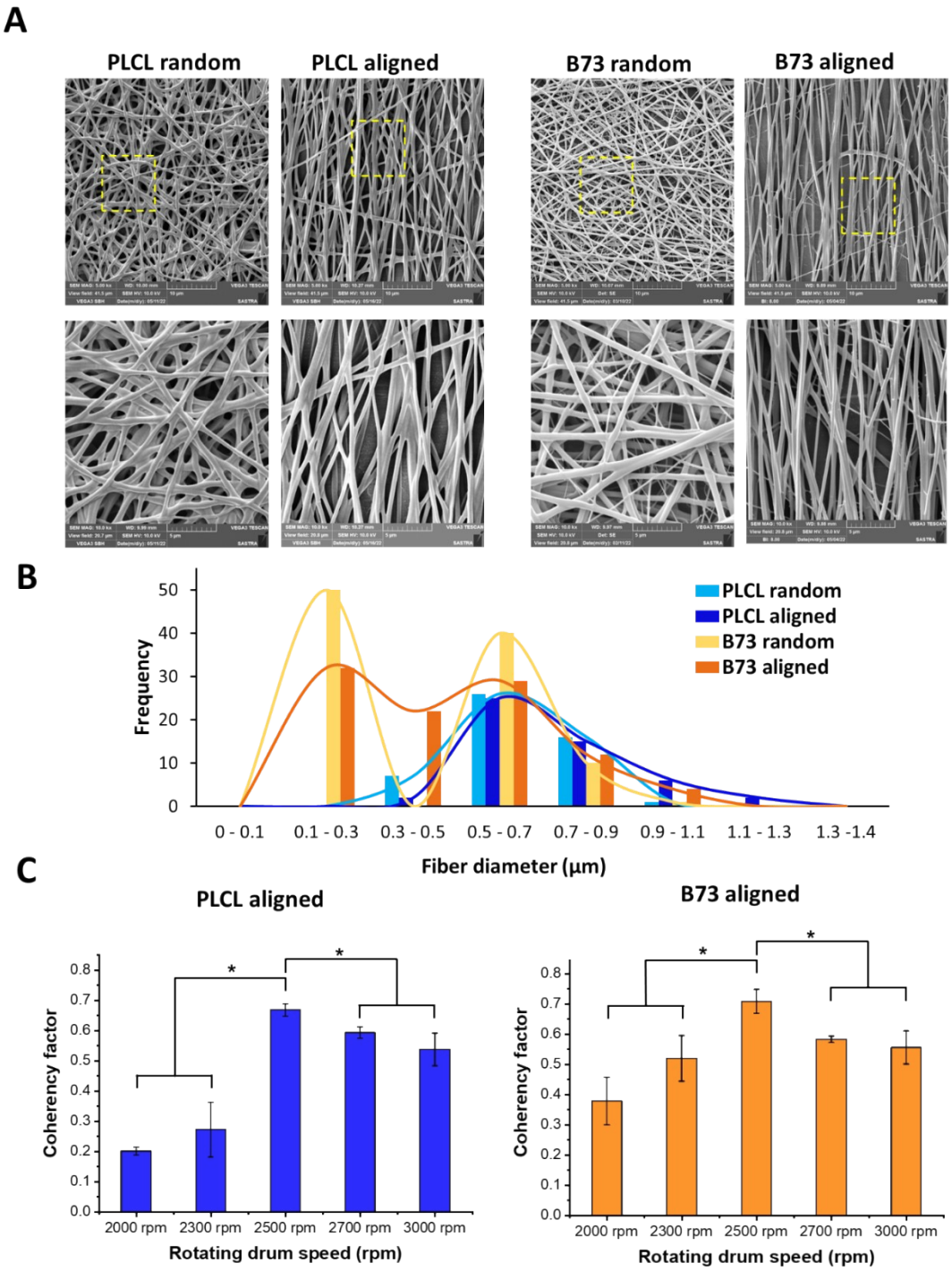


**Figure S1.** [A] Low (5,000X) and high magnification (10,000X) SEM images of the electrospun PLCL random, PLCL aligned, B73 random and B73 aligned nanofibers at the optimized electrospinning condition. [B] Histogram plot of fiber size distribution. [C] Coherency factor plot for PLCL aligned and B73 aligned for varied rotating drum speed.

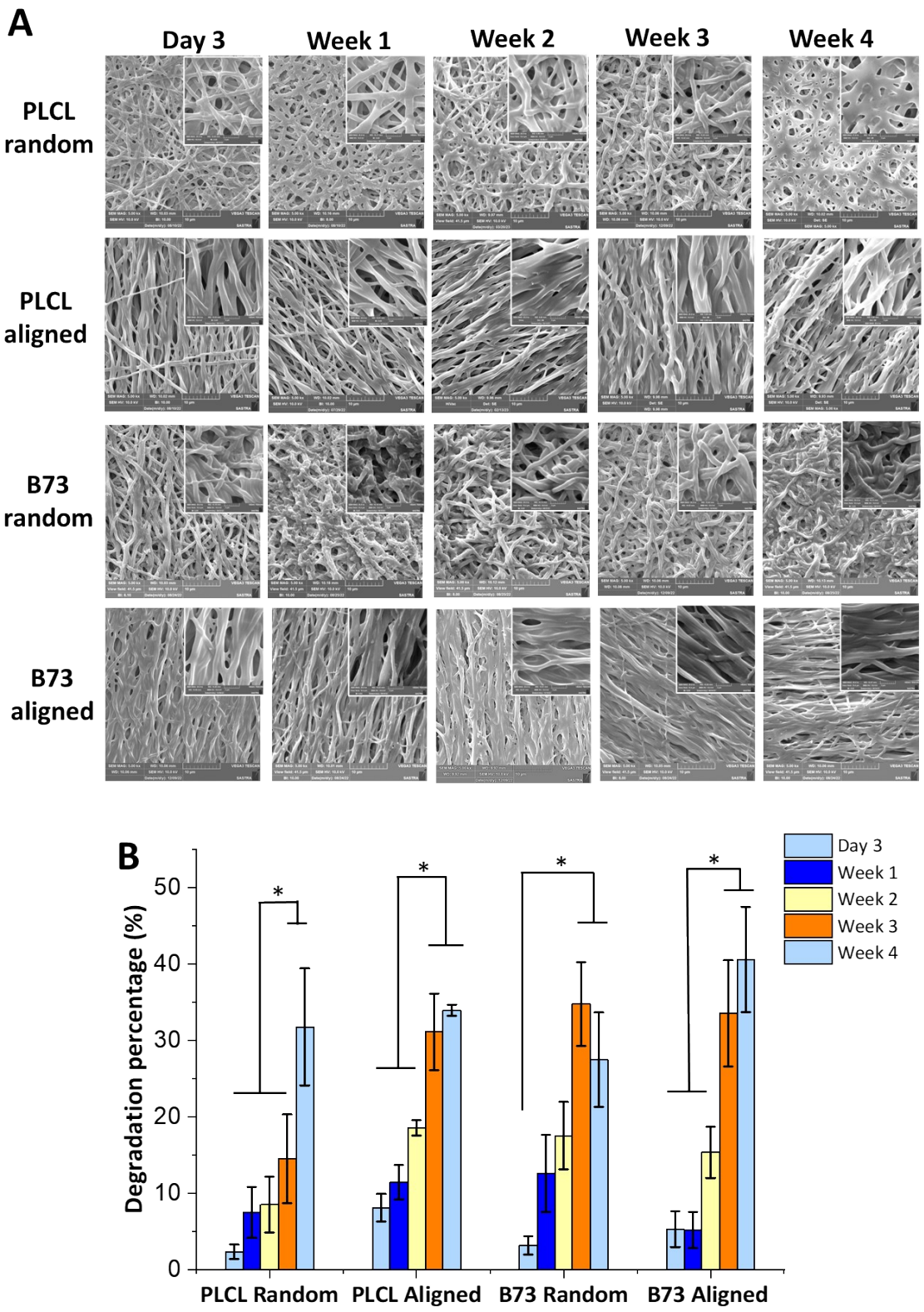


**Figure S2.** [A] Low (5,000X) and high (20,000X) magnification SEM images of the degraded nanofiber samples at different time points: day 3, week 1, week 2, week 3 and week 4. [B] Degradation percentages plot of PLCL random, PLCL aligned, B73 random and B73 aligned nanofibers from day 3 to week 4. (scale bar: 10 µm & 1 µm) (*$p<0.05$).

**S1. *In Vitro* Studies on Nanofibrous Support Matrix Using NRVCMs**

In this study, the cardiac regeneration potential of the developed aligned hydrophilic B73 nanofiber matrix was assessed by culturing NRVCMs for two weeks. The advantages of B73 blend nanofibers in promoting cardiomyocyte adhesion, migration and proliferation were analyzed and compared with the PLCL nanofiber matrix. Supplementary Fig. S3A shows the SEM images of the cultured nanofiber support matrix, illustrating the cell morphology after 3, 7 and 14 days of culture. At day 3, only a limited number of cells adhered to the surface of the nanofibers. However, the cell morphology was well elongated on aligned nanofibers and as the culture time increased, there was an increase in the number of cells that attached to the fiber surface with enhanced interactions among the cells. On day 7, the number of cells adhered to the nanofibers increased and on day 14, a layer of interconnected cell-cell networks was observed. Although the cell adhesion, migration, extensions and cell-cell interactions were found on all the nanofiber surfaces, aligned PLCL and B73 nanofibers demonstrated a distinct orientation in cell morphology and alignment along the fiber axis, resulting in improved cell migration and communication. Further, live/dead staining of the nanofibers on day 14 (Supplementary Fig. S3B) confirmed better viability of the NRVCMs due to the absence of dead cells on all nanofibers.

The MTS results confirmed an increase in cell proliferation from 3 to 14 days of culture in all experimental groups, confirming the nontoxic nature of the support matrix for potential use as a cardiac patch (Supplementary Fig. S3C). On the $14^{th}$ day, TCPS showed a higher rate of cell proliferation than all the nanofiber groups. However, there was no significant difference in cell adhesion, viability and cell proliferation among the nanofiber groups, while both aligned PLCL and B73 nanofibers showed improved cell orientation contributing to the development of cardiac anisotropy features.

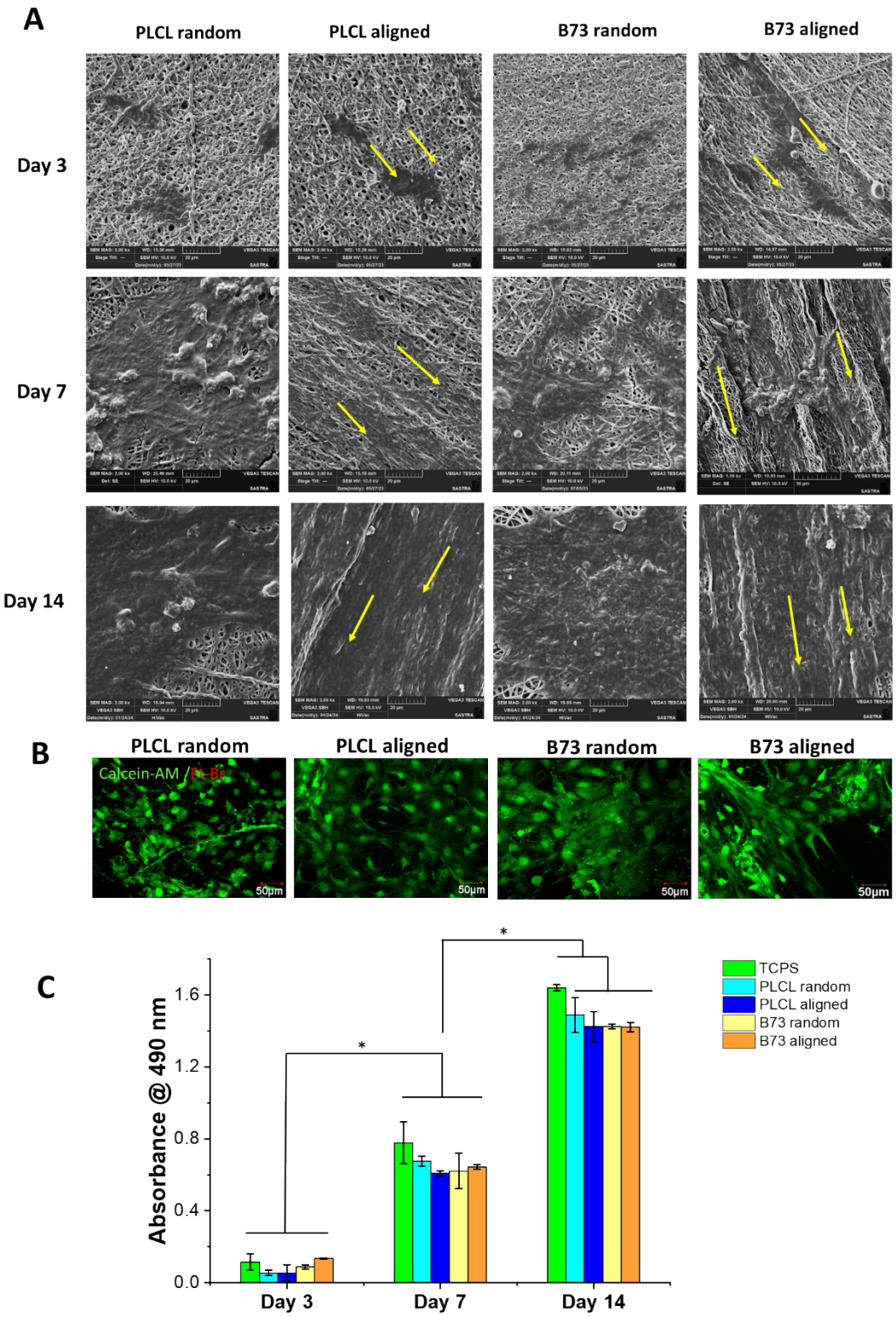


**Figure S3.** [A] SEM images of NRVCMs attached on the surface of nanofibers (arrows indicate the orientation of cell body along the fiber axis) (scale bar: 20 µm). [B] 2D multi-stack confocal images of the live/dead stained NRVCMs on nanofibers at day 14 (live - green & dead - red) (scale bar:50 µm). [C] Quantitative assessment of NRVCMs proliferation on nanofibers (*$p<0.05$).

Further, to evaluate the effect of nanofiber on improving cardiomyocyte elongation and maturation, immunofluorescence staining of F-actin, Cnx-43 and CTn-T expression was performed. The expression of connexin-43 (gap junction protein) confirmed the presence of cell-cell electrical coupling [1]. Supplementary Fig. S4A shows the phalloidin (F-actin) expression on all nanofibers, while both the random and aligned fibers exhibited well-organized actin expression mimicking native cardiomyocyte organization. Supplementary Fig. S4B shows the positive expression of the Cnx-43 surface marker in the cultured NRVCMs, showing the occurrence of cell-cell electrical coupling for contractile activity. Further, positive expressions of CTn-T on nanofibers confirmed the cardiac muscle fiber striation, indicating cardiomyocyte functionality (Supplementary Fig. S4C). These results confirmed the effective usage of B73-aligned nanofiber as a support matrix for the growth and maturation of cardiomyocytes. Recently, Taylor *et al.,* have developed an aligned reduced graphene oxide (PU-rGO) doped polyurethane fibrous scaffold for cardiac regeneration. It combines the effect of elasticity, conductivity and biocompatibility to improve cardiomyocyte functionality, aiding in the treatment of cardiac disease. *In vitro* studies on electrospun PU-10% rGO membrane using NRVCMs and hiPSC-CM confirmed enhanced cell elongation, growth and maturation through CCK-8 assay and immunofluorescence staining of cardiac markers (connexin 43, α-actin and troponin-T) [2].

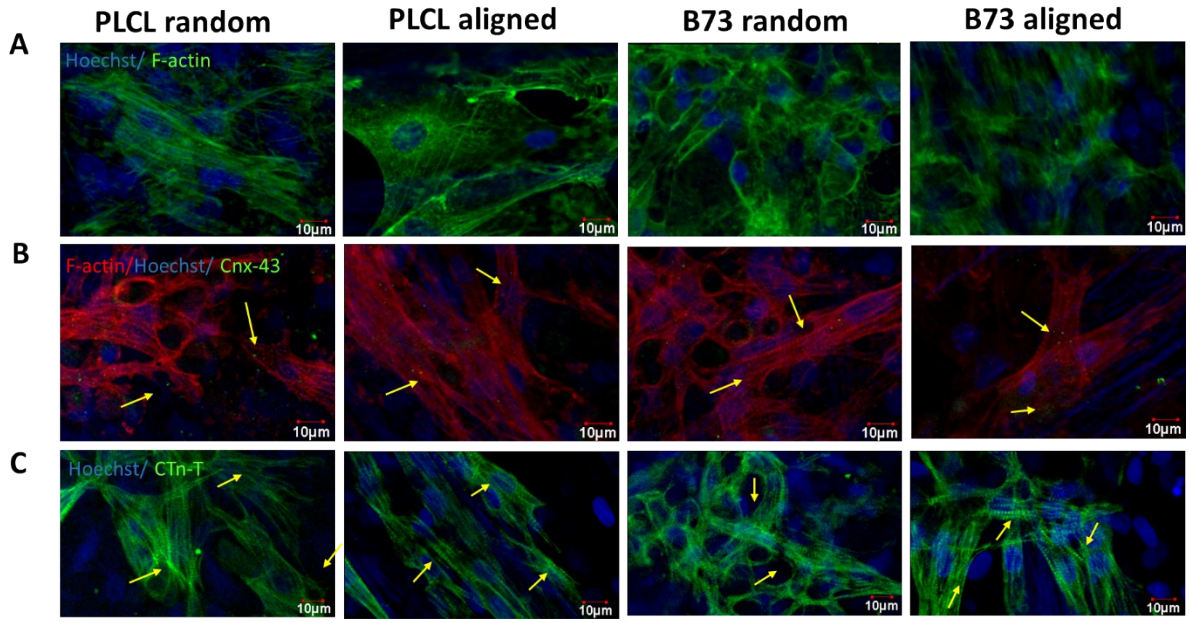


**Figure S4 .** 2D multi-stack confocal images of the stained NRVCMs cultured on random PLCL, aligned PLCL, random B73 random and aligned B73 nanofiber scaffolds after 14 days of culture. [A] Phalloidin (F-actin - green) & Hoechst (nucleus-blue) staining (scale bar: 10 µm), [B] Immunostaining of F-actin (red), Hoechst (nucleus-blue) and cardiac-specific markers Cnx-43 (green) and [C] Immunostaining of CTn-T (green) and Hoechst (nucleus - blue) (scale bar: 10 µm) (Yellow arrow indicate the presence of cardiomyocyte striations).

### S1.1. Quantification of NRVCMs Beating and Calcium Imaging

The mechanical properties of scaffolds that support cardiac contractile function are critical elements in scaffold design. A nanofibrous cardiac patch created for MI provides essential mechanical support to the dilated heart, improving its functionality by lessening ventricular dilation, lowering wall shear stress and contributing to the stability of the ventricular cavity [3]. The *in vitro* investigation of the cardiac contractile activity may provide a preliminary assessment of the developed scaffold for cardiac tissue engineering applications. Primary NRVCMs that resumed their contractile activity on scaffolds were assessed using video recordings and the fluo-4 AM calcium imaging technique. After 3 days of seeding (cell density of 1 x $10^5$ cells/scaffold), phase contrast microscope videos revealed that the cells on the random PLCL, aligned PLCL, random B73 and aligned B73 nanofiber support matrices were all visibly exhibiting beating activity. Synchronous beating was noted until day 7, during which

a video (AVI file) was recorded to quantify the cell beating data via a MATLAB algorithm. On day 7, the beating rates on random PLCL, aligned PLCL, random B73 and aligned B73 were found to be similar, at 36.8 ± 2.4, 37 ± 1.4, 38.7 ± 2.0, and 40 ± 2.6 bpm respectively (Supplementary Fig. S5B). The cardiomyocytes beating on PLCL random, PLCL aligned, B73 random and B73 aligned nanofibers at day 7 are presented as supplementary videos SV1, SV2, SV3 and SV4. This result confirmed the highly flexible nature of the PLCL & B73 electrospun fiber matrix that is appropriate for the rhythmic contraction and relaxation of cardiac tissue. Additionally, the use of a hydrophilic aligned nanofiber support matrix of B73, does not hinder cardiomyocyte functionality, as it maintains a functionality profile akin to that of PLCL nanofiber. Liang *et al.,* have also observed similar beating values for the NRVCM seeded 5% silk fibrnoin: 15% polypyrrole (7PPy15) nanofiber cardiac patch until day 8. From day 5, visible contraction of NRVCMs was observed for 7PPy mat and it reached stable contraction with the average beating rate of 39 ± 8 bpm on day 7. The contractile nanofiber mat development with Young's modulus of 1.437 ± 0.044 MPa and conductivity of ~0.1 mS/cm enabled effective contractile functions of the seeded cells [4]. However, at longer culture periods, the observation of beating through phase contrast microscope was challenging. Hence, to verify the occurrence of NRVCMs beating on day 7 and day 10, real-time intracellular calcium fluctuations were examined through fluorophore-based fluo-4 calcium imaging, which assessed the efficiency of electrical signaling transmission across the cells. Supplementary Fig. S5A provides the fluorescence intensity plot ($F/F_0$) representing dynamic calcium movement in the nanofibers. In summary, intensity plots were generated for three distinct regions of interest (ROIs) selected from a 60-second time-lapse video. The observed fluorescent signal from fluo-4 staining (a calcium indicator) facilitated the monitoring of transverse calcium movement in NRVCMs. Comprehensive quantification of these contractile characteristics, including total number of peaks and peak-to-peak distance values detected in various areas,

was done using a custom MATLAB algorithm. In all the groups, the NRVCM beating rate remained consistent on day 7 and 10, which ranged from 9 to 13 bpm during the 60-second observation period, thereby confirming the uniformity of cell beating on the cultured scaffold surfaces (Supplementary Fig. S5C). The peak-to-peak distance (time to peak) indicated the duration of calcium transition within a population of NRVCMs. Thus lower time to peak value signifies the presence of a highly interconnected cardiomyocyte population. After 7 days of culture, the time to peak values for random PLCL, aligned PLCL, random B73 and aligned B73 nanofiber were 5.4 ± 0.8, 4.8 ± 0.7, 5.4 ± 1.2, and 5.4 ± 0.7 seconds, respectively. Further, on day 10, the values were 5.2 ± 0.6, 5.1 ± 0.4, 4.7 ± 0.5 and 4.7 ± 0.5 seconds, respectively. This data revealed that there were no significant differences in the time to peak value on day 7 and day 10, which confirmed similar synchronous contractile behavior of NRVCMs on the fabricated electrospun support matrix [5]. On day 10, the signal intensity of the calcium ion was significantly reduced due to a decline in cardiomyocyte beating rate upon long term culture [6]. The captured calcium fluorescence signals on day 7 and day 10 for random PLCL, aligned PLCL, random B73 and aligned B73 nanofiber are presented as supplementary videos (Supplementary Videofile SV5 to SV12). Subsequent calcium fluorescence imaging of NRVCMs confirmed that calcium ion movement was uniformly oriented with the fiber direction on the aligned scaffold whereas random movement of calcium ions was noted on the random scaffolds. This is because of the anisotropic cellular elongation with unidirectional contractile cardiomyocyte maturation along the fiber axis on aligned nanofibers. These observations demonstrated that the aligned B73 hydrophilic nanofiber support matrix could improve cardiomyocyte contractility.

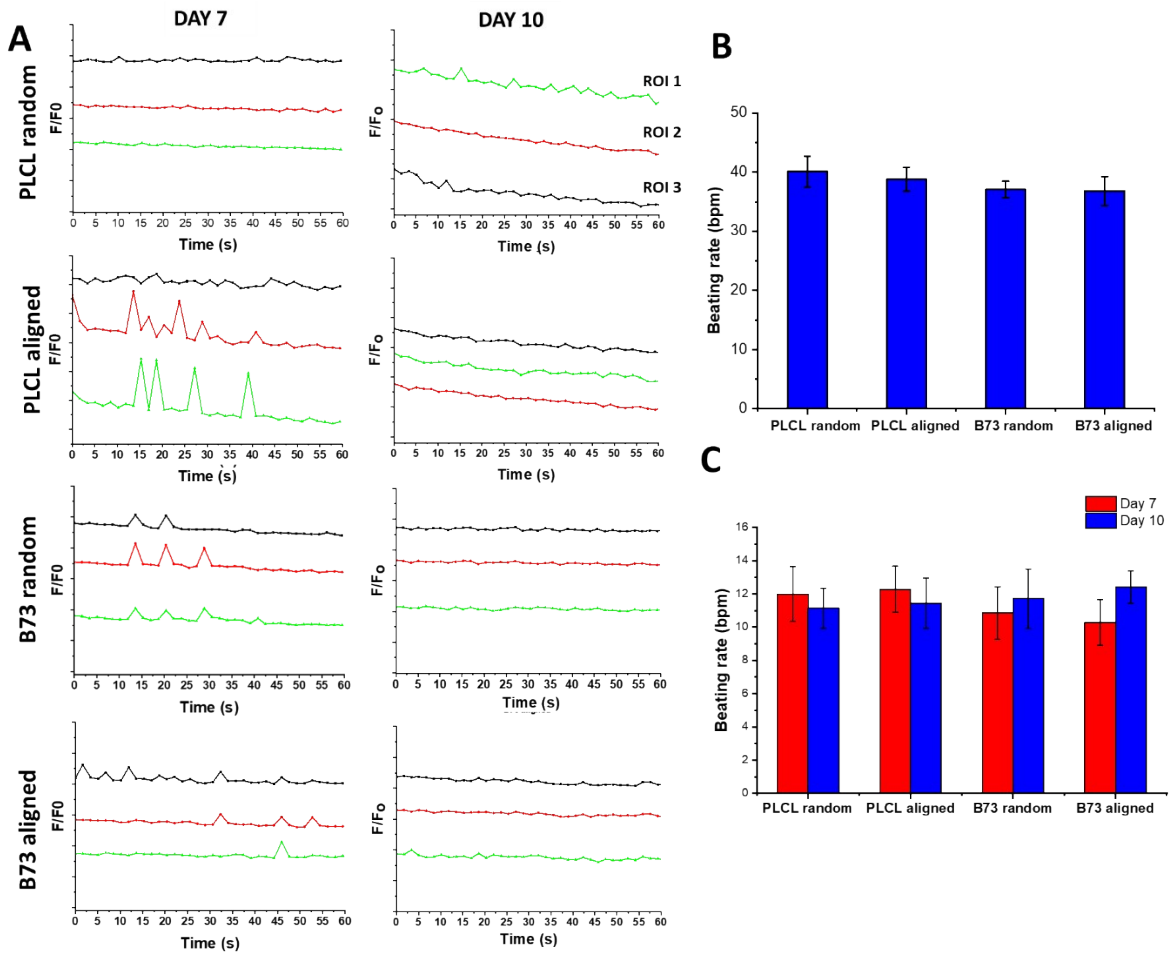


**Figure S5.** [A] Fluorescence intensity plot ($F/F_0$) of $Ca^{2+}$ signal from NRVCMs cultured on nanofibers. Quantification of NRVCMs beating on nanofiber using programmed MATLAB codes from video recordings obtained using [B] Optical microscope and [C] Confocal microscope.

## S1.2. Gene Expression Analysis

The functionality of cardiomyocytes cultured on scaffolds was assessed by RT-qPCR gene expression analysis. Connexin 43 serves as a gap junction protein that supports intercellular calcium transfer, thereby enhancing electrical signal propagation, ensuring synchronized coupling during cardiomyocyte activity. Cardiac α-sarcomeric actin is a contractile protein & a responsible structure for cardiac myofilaments to perform contraction and relaxation [7]. Although significant differences were not observed in the cell proliferation rate on PLCL and B73 nanofibers, the RT-PCR study could highlight the functional differences among the

groups. The expression levels of both α-actin and Cnx-43 were elevated on day 7 of the culture however, a significant decline in gene expression was observed on day 14. This observation correlates with the beating analysis data obtained through fluo 4 AM calcium imaging, which indicated a reduction in signal intensity on day 10, suggesting a lower concentration of calcium transition in the cardiomyocyte population cultured on the nanofibers. The expression of Cnx-43 in the B73 aligned nanofiber support matrix exhibited a significant increase, with a fold change of 2.50 ± 0.05 on day 7, in comparison to other nanofiber matrices (Supplementary Fig. S6). This result indicated the presence of a highly interconnected population of cardiomyocytes with active calcium ion movement. Regarding α-actin expression on day 7, the PLCL aligned matrix showed a significant increase in fold change of 0.56 ± 0.12, in contrast to the PLCL random mat, which exhibited a fold change of 0.33 ± 0.02. On day 14, Cnx-43 expression was significantly reduced on all nanofibers, indicating reduced beating activity during prolonged culture duration. Notably, both the random and aligned B73 nanofiber matrices presented a comparable α-actin expression profile of 0.55 ± 0.04 and 0.45 ± 0.01 fold change, respectively, which was similar to the aligned PLCL matrix on day 7. The α-actin expression on day 14 was significantly reduced on all nanofibers compared to day 7. The reduced α-actin expression can be correlated with the reduced NRVCM beating activity during the prolonged culture period (10 days). The gene expression study confirmed the effective functional restoration of NRVCMs growth on the nanofiber B73 aligned support matrix.

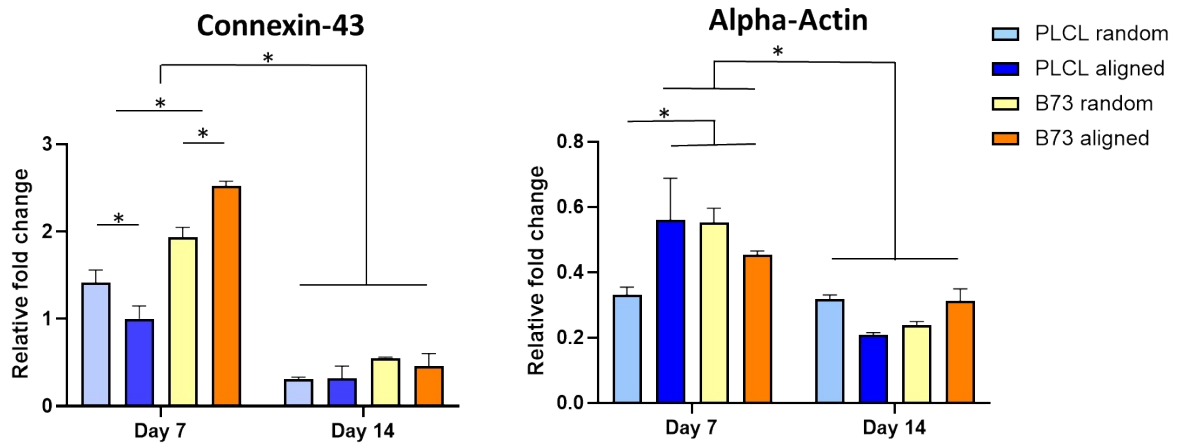


**Figure S6.** Expression profiles of the connexin 43 and α-actin genes at day 7 and day 14 on the nanofiber surface. (*p<0.05).

**Table S1**. Physicochemical characteristics of electrospun fibers, such as fiber diameter (μm), contact angle (°), porosity (%), Young's modulus (MPa), UTS (MPa), elongation percentage (%), and degradation percentage (%).

| Properties | PLCL random | PLCL aligned | B73 random | B73 aligned |
|---|---|---|---|---|
| **Diameter** | 548 ± 130 nm | 624 ± 185 nm | 492 ± 81 nm<br>123 ± 22 nm | 529 ± 118 nm<br>182 ± 47 nm |
| **Contact angle** | 96 ± 5°<br>hydrophobic | 78.3 ± 7°<br>hydrophobic | 21 ± 4°<br>hydrophilic | 22 ± 4°<br>hydrophilic |
| **Porosity** | 90 ± 3% | 93 ± 3% | 88 ± 13% | 91 ± 5% |
| **Young's Modulus** | 1.8 ± 0.3 MPa | 5.2 ± 0.5 MPa | 1.5 ± 0.1 MPa | 9.9 ± 2.3 MPa |
| **Ultimate tensile strength (UTS)** | 3.8 ± 1 MPa | 4.7 ± 0.5 MPa | 2 ± 0.2 MPa | 10.2 ± 2.1 MPa |
| **Elongation percentage** | 157.1 ± 21.1% | 199.7 ± 42.7% | 45.3 ± 16.5% | 228.2 ± 53.8% |
| **Degradation @ week 4** | 31.8 ± 7.6% | 34 ± 0.7% | 27.5 ± 6.2% | 40.6 ± 6.9% |

## Supplementary References


1 M. Khan, Y. Xu, S. Hua, J. Johnson, A. Belevych, P. M. L. Janssen, S. Gyorke, J. Guan and M. G. Angelos, *PLoS One*, 2015, **10**, 1–19.

2 A. Taylor, J. Xu, N. Rogozinski, H. Fu, L. Molina Cortez, S. McMahan, K. Perez, Y. Chang, Z. Pan, H. Yang, J. Liao and Y. Hong, *ACS Biomater Sci Eng*, 2024, **10**, 3759–

3774.

3 M. Nguyen-Truong, Y. V. Li and Z. Wang, *Bioengineering*, 2020, **7**, 1–24.

4 Y. Liang, A. Mitriashkin, T. T. Lim and J. C. H. Goh, *Biomaterials*, DOI:10.1016/J.BIOMATERIALS.2021.121008.

5 Y. He, G. Ye, C. Song, C. Li, W. Xiong, L. Yu, X. Qiu and L. Wang, *Theranostics*, 2018, **8**, 5159–5177.

6 X. Wang, L. Wang, Q. Wu, F. Bao, H. Yang, X. Qiu and J. Chang, *ACS Appl Mater Interfaces*, 2019, **11**, 1449–1468.

7 J. Meng, B. Xiao, F. Wu, L. Sun, B. Li, W. Guo, X. Hu, X. Xu, T. Wen, J. Liu and H. Xu, *Mater Today Bio*, DOI:10.1016/j.mtbio.2022.100415.